Nanoscale

REVIEW

View Article Online
View Journal | View Issue

Cite this: *Nanoscale*, 2025, **17**, 3671

Biomolecular ligands as tools to modulate the optical and chiroptical properties of gold nanoclusters

Laura Saa, [a] Manuel Núñez-Martínez,[a] Eva Carpintero-Cueto[a,b] and Aitziber L. Cortajarena *[a,c]

Received 15th October 2024,
Accepted 8th December 2024

DOI: 10.1039/d4nr04267k

rsc.li/nanoscale

Biomolecule-stabilized gold nanoclusters (AuNCs) have become functional nanomaterials of interest because of their unique optical properties, together with excellent biocompatibility and stability under biological conditions. In this review, we explore the recent advancements in the application of biomolecular ligands for synthesizing AuNCs. Various synthesis approaches that are employing amino acids, peptides, proteins, and DNA as biomolecular scaffolds are reviewed. Furthermore, the influence of the synthesis conditions and nature of the biomolecule on the emerging optical (absorption and photoluminescence) and chiroptical properties of AuNCs is discussed. Finally, the latest research on the applications of biomolecule-stabilized AuNCs for biosensing, bioimaging, and theranostics is presented.

Introduction

Gold nanoclusters (AuNCs) consisting of a few to hundred atoms of sizes below 2 nm are considered intermediates between gold nanoparticles (AuNPs) and isolated molecules.[1] This feature confers AuNCs with different photophysical properties, such as strong absorption and photoluminescence, compared to the AuNPs.[2] In this type of ultrasmall nanomaterials, the motion of free electrons is restricted to a confined space having discrete electronic bands (Fig. 1A). Thus, quantum confinement effects govern AuNCs, providing them with interesting electronic and optical properties and thereby attracting the scientific community to explore these materials. For this reason, in the past few years, numerous nanomaterials based on AuNCs with applications in imaging,[3] sensing,[4] catalysis[5] and energy conversion[6,7] have been developed.

For the synthesis of AuNCs, two main protocols are reported in the literature; top-down and bottom-up approaches. Top-down strategies involve the use of etching ligands (*e.g.*, sulfhydryl compounds) and etching solvents. By employing the etching approach on a gold core, various types of AuNCs could be produced.[8] For the bottom-up approach, gold ions are incubated in the presence of protecting agents and then reduced either at a high pH or by adding a strong ($NaBH_4$) or mild (citrate or ascorbic acid) reducing agent. In the resulting nanomaterial, protecting ligands constitute a crucial element because in addition to preventing the natural aggregation of the gold atoms, they modulate the emerging physical and chemical properties, such as biocompatibility,[4] chirality,[9] and solubility. Thus, the literature reports on AuNCs protected by different coating agents. The scientific community has also given considerable attention to the covalent bond between the ligand and the gold atoms.[10] For instance, the use of small thiolated (Au–S)[11] and phosphine (Au–P)[12] molecules, which enable the preparation of atomically precise AuNCs, has been extensively investigated. Additionally, biomolecules, such as amino acids, peptides, proteins, or DNA, can be used as biotemplates of AuNCs (Fig. 1B). The presence of these bioligands on the surface of AuNCs enables combining their interesting features, including aqueous solubility or biocompatibility, with the optical properties of the AuNCs. This strategy enables the creation of novel nanobiomaterials for application in biomedical and biotechnological fields.[13,14]

Combining various types of biomolecular protection with metallic cores can result in nanostructured biomaterials with a range of features, which can be tuned for a specific biological functionality. For this reason, exploring and understanding the key factors that govern the emerging photophysical characteristics of the NCs in these systems are crucial. These investigations aim to achieve precise control over the optical and chiroptical characteristics of nanomaterials, allowing for the development of materials with specific and desirable properties.

In this review, we highlight the optical and chiroptical properties of AuNCs stabilized by biological ligands, with a special focus on the main strategies to obtain fluorescent

[a]*Center for Cooperative Research in Biomaterials (CIC biomaGUNE), Basque Research and Technology Alliance (BRTA), Donostia-San Sebastián, 20014, Spain. E-mail: alcortajarena@cicbiomagune.es*
[b]*University of the Basque Country (UPV/EHU), 48940 Leioa, Spain*
[c]*Ikerbasque. Basque Foundation for Science, Bilbao, 48009, Spain*

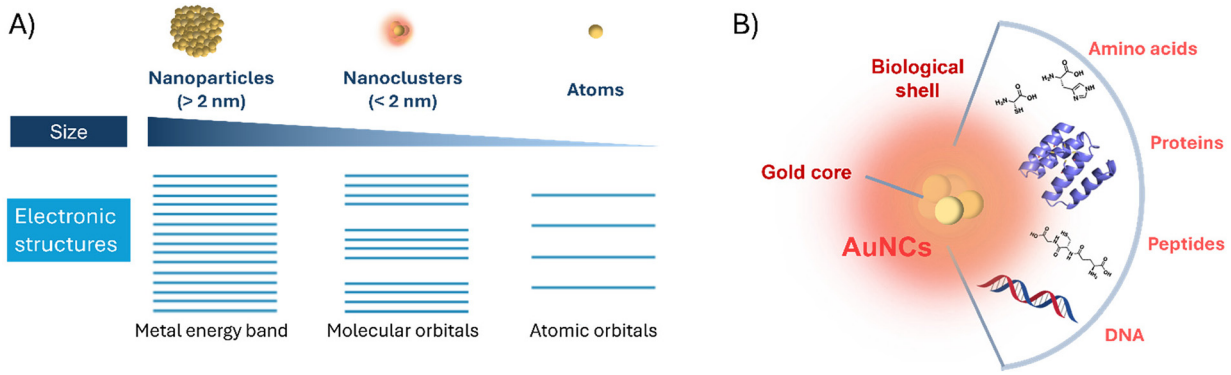

Fig. 1 (A) Size-dependent electronic structure of metal nanomaterials showing gold nanoparticles with continuous electronic bands and gold nanoclusters with discrete energy bands. (B) Different biological molecules, such as amino acids, peptides, proteins or DNA, used as protecting agents in the synthesis of metal nanoclusters.

AuNCs using natural biomolecules – amino acids, peptides, proteins, and DNA. We also discuss the different factors affecting the optical and chiroptical features of these nanomaterials. In the second part, we describe recent examples of bio-templated AuNCs and their applications in biosensing, biotechnology, bioimaging, and theranostics.

Optical properties of AuNCs

AuNC materials are commonly prepared by reducing Au(III) in the presence of suitable reducing and capping agents. The presence of appropriate ligands is required to control the growth of the nanostructures and, thus, prevent them from aggregation and NP formation. Thiolated molecules are the most preferred ligands due to the strength of the Au–S bond, and significant research has been conducted to prepare AuNCs with a precise number of gold atoms, defined atomic structures, and unique physical and chemical properties.[9,15–18]

AuNCs exhibit molecule-like properties induced by discrete electronic transitions. The discrete energy levels and the corresponding HOMO–LUMO transitions lead to size-dependent emission properties.[19] In this sense, AuNPs (size >2 nm) do not present the photoluminescence properties commonly found in AuNCs with a size of <2 nm (Fig. 1A). Moreover, AuNP dispersions show surface plasmon resonance bands, whereas NCs do not exhibit a plasmonic behaviour. AuNCs exhibit size-dependent excited state and electron transfer properties, with their optical and electronic properties varying greatly with the exact metal atom number and coordinating ligands.[20] As the size of the nanomaterial approaches 2 nm, the quantum confinement effect becomes significant, inducing fascinating optical behaviors such as luminescence, discrete electronic transitions, molecular-like relaxation of the excited state, two-photon absorption, photothermal conversion, and photodynamics.[21,22] Among these optical properties, their strong photoluminescence, compared to other metal nanomaterials, is one of the most interesting features due to its potential applicability in different fields. Although extensive research has been performed,[21] the mechanisms underlying the photoluminescence of AuNCs are still not fully understood. Still, this phenomenon has been attributed to ligand-to-metal charge transfer (LMCT) or ligand-to-metal–metal charge transfer (LMMCT) from the ligand to the Au core, followed by radiative relaxation. Thus, core composition and structure, as well as protecting ligands for AuNC stabilization play an important role in the modulation of the photoluminescence properties. In this sense, Wu *et al.* have demonstrated that the fluorescence intensity of Au_{25}NCs was highly affected by a charge transfer phenomenon from the ligands to the AuNCs. Remarkably, they found that the fluorescence properties of AuNCs can be modulated by increasing the ligand's capability of donating charges using ligands with electron-rich atoms (*e.g.* S, N, and O) or functional groups (*e.g.* $-NH_2$ and $-COOH$).[23]

Synthesis of biomolecule-stabilized AuNCs and modulation of their optical properties

As previously indicated, both the synthesis conditions and the molecular nature of stabilizing ligands play a crucial role in determining the photophysical properties of biotemplated nanomaterials. As a result, extensive research has been conducted to unravel the influence of these elements to precisely control the creation of biohybrid materials with the defined optical characteristics.[24–26] Herein, we summarize the last research developed in the use of amino acids, peptides, proteins and DNA as molecular scaffolds for the synthesis of AuNCs (Fig. 1B).

AuNCs stabilized by amino acids

Due to the complexity of the chemical structures and conformational space of proteins used as biological templates, studying the effects of protein primary, secondary and tertiary structures on photoluminescence mechanisms remains a challenge.

Understanding the atomic-level structure and assembly of AuNCs within protein molecules is crucial for elucidating the mechanisms behind the modulated emission brightness and for guiding future developments in sensing and imaging applications. Therefore, to shed light on the role of individual amino acids in the anchoring, reduction of metal ions, and stabilization of the metal core within proteins, investigations on the interactions between free amino acids and Au(III) were performed.[27] Cysteine (C) and Histidine (H), as well as negatively charged amino acids glutamate and aspartate, bind preferentially Au(III). Regarding the reduction potential, cysteine, methionine (M), and tyrosine (Y) exhibit a high tendency to reduce Au(III) to Au(I).

Bélteki *et al.* investigated the role of L-phenylalanine (F), L-glutamine (Q), and L-arginine (R) as ligands for the synthesis of fluorescent AuNCs under different experimental synthesis conditions such as amino acid/metal ion ratios, concentration of metals, pH, temperature and reaction time.[28] They highlighted the effect of these parameters on the photoluminescence intensity, quantum yield (QY), and fluorescence lifetime (τ). The use of high ligand excess during the synthesis ensures the appropriate reduction of metal ions, the stabilization of the formed clusters, and the formation of surface functional groups. The synthesis process will vary depending on the reducing capability of the ligands, which determine the amount of Au(0) in the NC core, and as a result, their optical features. Electron-rich functional groups in the side chain of arginine facilitate photoluminescence enhancement, and a QY up to 15–18% was obtained. Fluorescence lifetimes showed increased values depending on the chosen amino acid, according to the following order: phenylalanine < arginine < glutamine (Fig. 2A). In the case of glutamine, this effect is attributed to the uncharged side chain, with electron-withdrawing moieties, which involves a rigidification of the structure, and consequently, longer lifetime values. AuNCs exhibiting different emission wavelengths can be generated by changing the capping amino acid. For example, blue,[29] orange[30] and yellow-green fluorescence[31] have been obtained using tryptophan, methionine, and tyrosine as stabilizing ligands, respectively.

AuNCs stabilized by peptides

Due to its small size and high biocompatibility, the tripeptide glutathione (GSH) has been widely used as a capping ligand for AuNC fabrication.[20,32,33] GSH possesses a thiol group that can effectively bind to the surface of gold, ensuring the stability of AuNCs and preventing them from aggregation. The number of gold atoms in the core and GSH molecules in the shell influences the photophysical and photocatalytic behaviour of these AuNCs. The size-dependent excited state of AuNCs protected with glutathione was studied by Stamplecoskie *et al.* In this work, the authors demonstrated that the excited properties of AuNCs depend on their size. For larger NCs, a predominant excited-state relaxation that occurs within picoseconds is evident, attributed to metal–metal tran-

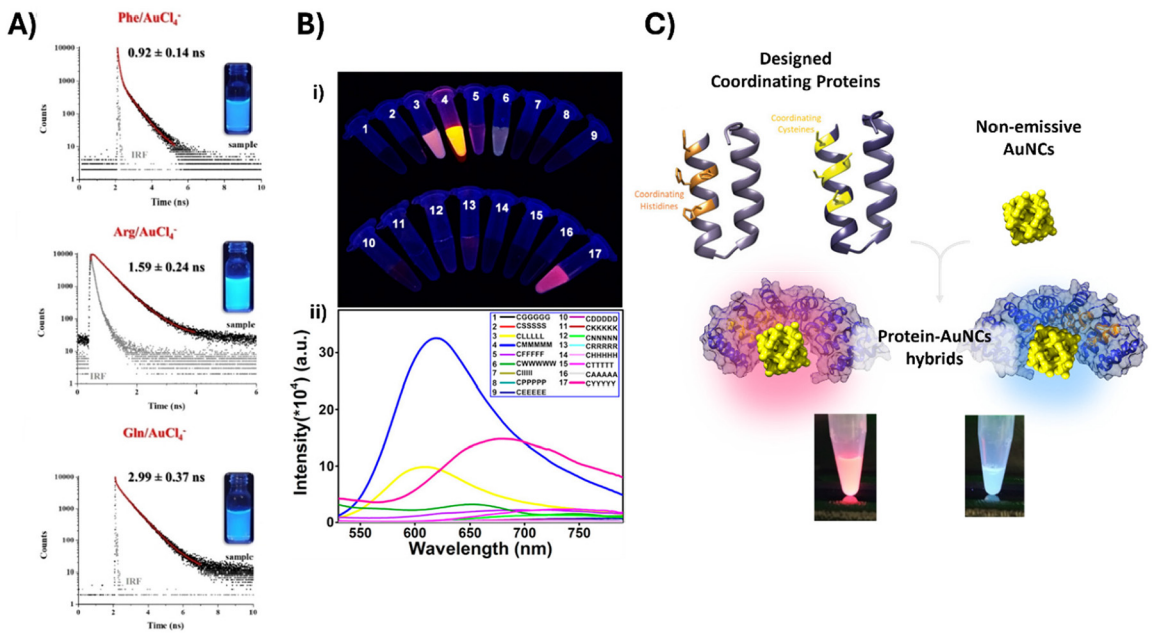

Fig. 2 Influence of biomolecular ligands (amino acid, peptide, and proteins) on the optical properties of AuNCs: (A) fluorescence decay profiles, average lifetime values and pictures under UV-light of phenylalanine-, arginine-, and glutamine-stabilized AuNCs. Reproduced from ref. 28 with permission from Wiley-VCH GmbH, copyright 2023. (B) Sequence-based modulation of fluorescence of peptide-AuNCs. (i) Photographs of the AuNC template with different peptide sequences under UV light. (ii) Fluorescence emission spectra of the AuNC template with different peptide sequences. Reproduced from ref. 38 with permission from the American Chemical Society, copyright 2019. (C) Schematic of the designed CTPR proteins for the coordination of metal naked NCs including the pictures of histidine- or cysteine-based resulting hybrid materials under UV-light. Reproduced from ref. 60 with permission from Wiley-VCH GmbH, copyright 2021.

sitions, followed by a long-lived scale lifetime of nanoseconds. Small GSH-AuNCs, due to a reduced number of core metal atoms, behave like gold complexes. No sub-picosecond relaxation was observed in this case, and ligand–metal charge transfer states dominate the relaxation dynamics.[20]

In addition to the importance of the gold core structure in the optical properties of AuNCs, recent studies have highlighted that the amino acid sequence of peptide ligands plays an important role in determining the surface peptide structuring, interfacial water dynamics, and ligand–Au core interaction. Moreover, peptide aromaticity, hydrophobicity, electron-donating capacity, and solution pH are all crucial factors that influence the emission features of AuNCs.[34]

Dai *et al.* explored the mechanism and peptide ligand effect on the Stokes shift.[35] Rationally designed tripeptides with modulated sequences were used to synthesize a series of fluorescent AuNCs with Stokes shifts up to 530 nm, with potential applications in bioimaging due to their emission in the near-infrared (NIR) region. It was observed that protecting ligands consisting of tyrosines and cysteines (sequence: Y–C–Y) led to a more significant Stokes shift than the other amino acid compositions, which can be explained by an aromatic ligand-mediated two-step Förster resonance energy transfer (FRET) mechanism. It was shown that the energy absorbed by the tyrosines can be effectively transferred by this process and released as fluorescence emission in the NIR fluorescence range.

A combination of computational simulations and experimental studies revealed the role of the peptide within the stabilizing shell structure and its interaction with the gold core in the optical properties of peptide-AuNCs, which additionally varied in response to pH changes.[36] It was described that changes in the hexapeptide sequence altered the electrostatic environment, affecting the deprotonation equilibrium of the peptide N-terminus in the proximity to the Au core, and thus the pH-responsive fluorescence intensity. A glycine (G) and aspartic (D)-containing CGGGDD-AuNCs peptide was found to be the most sensitive to pH changes, followed by other peptide sequences with valine (V) or tyrosine (CVVGDD and CYYGDD). Similarly, $CCYR_9$-AuNCs and CCYRKKRRQRRR-AuNCs showed different absorption and emission features. Although both compositions have red emissions under UV light in most pH ranges, $CCYR_9$-AuNCs displayed cyan fluorescence at a pH above 12.[37]

The screening of different peptides with a fixed cysteine terminal for the coordination with Au and stabilization of AuNCs revealed that the methionine-based peptide CMMMMM resulted in AuNCs with significantly stronger fluorescence than the other amino acid hybrids. This enhanced fluorescence can be explained by a higher content of emissive component Au(I) species, as determined by X-ray photoelectron spectroscopy (XPS) analysis, when compared to the tyrosine-based peptide CYYYYYY (Fig. 2B).[38]

AuNCs stabilized by proteins

Proteins are especially attractive as ligands for AuNC synthesis since they act as environmentally friendly reducing and stabilizing molecules while also offering natural biocompatibility.

Since the pioneering work reported by Xie *et al.* in 2009,[39] in which bovine serum albumin (BSA) was employed to prepare fluorescent AuNCs, a plethora of proteins have been used as scaffolds for the synthesis of fluorescent AuNCs. Ovalbumin,[40,41] papain,[42] glucose oxidase and horseradish peroxidase,[43] pepsin, trypsin and lysozyme[44] are some of the natural proteins that have been employed as biomolecular templates for the stabilization of AuNCs.

Despite being one of the most widely used methods for synthesizing fluorescent AuNCs,[45] the precise mechanism of the emissive properties of BSA-AuNCs still remains unclear. Recently, there has been an increased interest in understanding the specific mechanisms that govern the synthesis and photoluminescence of BSA-NCs.[46,47] In this sense, Chevrier *et al.*[48] performed synchrotron-based X-ray absorption fine structure (XAFS) spectroscopy, and rigidifying/unrigidifying experiments to investigate the structure and luminescence mechanism of the BSA-AuNCs, with the Au(I)–thiolate complexes being the proposed main structures found in these BSA-AuNCs. The investigations of the reducing and capping residues involved in the synthesis process showed that methionine and cysteine residues are responsible for Au reduction and AuNC growth. Additionally, among the 16 disulfide bonds within BSA, specific disulfide pairs C75–C91/C90–C101, C315–C360/C359–C368, and C513–C558/C557–C566 were identified as the potential NC nucleation positions within the BSA protein structure.[46] The correlation between the synthesis pH and the composition of the gold core was studied by Sun *et al.*[49] An increase in solution alkalinity to pH 12 during the synthesis procedure resulted in BSA-AuNCs with stronger absorption, decreased luminescence, and a lower Au(I)/Au(0) ratio than BSA-AuNCs synthesized at pH 11.5, which presented enhanced brightness and a significant increase in the Au(I) proportion. The concentration of NaOH and the addition time to the BSA solution have also been described as key factors in the formation and emission properties of BSA-AuNCs.[50] The combination of BSA with specific amino acids, along with variations in the pH of the reaction solutions, enabled the production of protein–Au hybrid nanomaterials with distinct fluorescence emission properties. These modulated optical features can be correlated with the different compositions of the gold core, specifically the Au(I)/Au(0) ratio.[51]

A thiol-rich copper storage protein was employed by Selvan and coworkers as a template to synthesize and stabilize red-emitting luminescent AuNCs.[52] The 13 cysteine residues located along the central helical core of the protein were intended to concentrate the thiolates, favouring the cluster formation. Biomineralization synthesis method, mediated by the endogenous reduction by the amino acids of the protein, led to AuNCs with higher quantum yields and higher Au(I)/Au(0) ratios than the AuNCs prepared by exogenous reduction with $NaBH_4$, illustrating again the key role of the scaffold.

Considering the reported examples using existing proteins, pre-engineered protein templates emerged as an effective strategy to achieve further control and modulation of the optical properties and cellular uptake of AuNCs.[53] As a first example,

chemically tailored BSA including an increased number of positive net charges (cBSA, *i.e.* cationic) or negative charges (aBSA, *i.e.* anionic BSA) were created by reacting the carboxyl and amino groups of BSA with ethylenediamine and succinic anhydride, respectively. Using these pre-modified variants for AuNC synthesis resulted in nanohybrids with different core sizes and distinctive photophysical characteristics. cBSA-AuNCs exhibited the smallest size and the brightest red emission under 365 nm light irradiation, while aBSA-AuNCs were larger and showed the weakest luminescence and shorter luminescence lifetimes than those of cBSA-AuNCs. In terms of cellular uptake, aBSA-AuNCs demonstrated a larger cellular uptake level than cBSA-AuNCs attributed to the fact that aBSA-AuNCs presented a more negative surface charge than those stabilized with the cBSA variant, according to the Z-potential measurements.

Alternative approaches such as the post-synthesis functionalization of BSA-AuNCs with cysteine and tyrosine-containing polypeptides have also proven to stabilize the AuNCs and enhance their PL properties.[54] These reported pre- or post-modification strategies provide certain flexibility and versatility in the design and fabrication of functional luminescent bionanomaterials. Nevertheless, chemical modification of the proteins is a rather limiting approach, allowing mainly the control of the overall physicochemical features and limited control over the sequence and structure of natural proteins. Thus, advancements in synthetic biology and protein engineering can accelerate the generation of metal-coordinating proteins that mimic natural metalloproteins and allow the precise design of biomolecular templates for the synthesis of AuNCs with defined optical features.[14] In this sense, Zang *et al.* engineered the specific ferroxidase center buried within the intrasubunit of ferritin to introduce cysteine residues, which can specifically bind gold. These modifications created a new compartment for the growth of fluorescent AuNCs, while keeping the functionality of the protein cavity. The as-synthesized AuNCs exhibited high stability given by the size-constrained ferroxidase centers buried within a four α-helix bundle, which prevents the excessive growth of AuNCs.[55] Beyond the engineering of natural proteins, designed repeat proteins have been investigated as effective templates for the synthesis and stabilization of metal nanomaterials, due to their modularity and easy sequence tunability. Couleaud *et al.* first demonstrated that consensus tetratricopeptide repeat (CTPR) proteins bearing a single cysteine could effectively stabilize AuNCs, resulting in the formation of red-emitting functional hybrid nanostructures.[56] Furthermore, protein engineering has been utilized to introduce metal-coordination sites into the CTPR protein template for the synthesis of highly luminescent AuNCs. Designed metal-binding sites based on histidine or cysteine residues facilitated the creation of protein–AuNC hybrids with excellent blue-emitting fluorescence properties,[57,58] while the cysteine-based scaffold produced AuNCs with dual emissions centered at 450 and 700 nm.[59] The introduction of tryptophan residues at specific positions enhanced photoluminescence properties due to the electron-rich protein environment provided by the Trps and the favourable energy transfer from Trps to AuNCs.[57] In another approach, water-dispersible AuNCs without organic ligands (termed naked AuNCs or AuNKNCs) were combined with CTPR proteins containing 16 histidine or cysteine coordinating residues, resulting in hybrids with distinct optical properties in terms of fluorescence emission and luminescence lifetimes[60] (Fig. 2C). These reports allowed the systematic exploration of the role of the protein template on the photophysical features of the resulting hybrids, since proteins with similar structures and a distinct coordinating environment allowed the fine-tuning of the emission wavelength, quantum yield, lifetime, and emission mechanisms.

AuNCs stabilized by DNA

As we mentioned in the introduction, protecting ligands present a fundamental role in the preparation of AuNCs avoiding their aggregation and further growth to NPs.[61] In this sense, DNA appears as an interesting biomolecule to act as a protecting agent of metal NCs. DNA molecules can interact with gold and silver metals through coordination with nitrogen atoms in the nucleobases. Adenine and cytosine have been reported to interact preferentially with gold atoms, while silver binds not only cytosine but also thymine and guanine.[62] Therefore, specific DNA sequences can be used to promote the formation of AuNCs or AgNCs resulting in nanohybrids with tunable emission characteristics. The preparation of DNA-stabilized AgNCs has been more extensively documented[63,64] than that of AuNCs. Still, the low toxicity and high stability exhibited by DNA-AuNCs make them good candidates for developing new bionanomaterials such as fluorescence emitters, catalysts, or antibacterial agents for biosensing, catalysis, or antimicrobial applications.

Various DNA molecules including single-stranded DNA (ssDNA) and double-stranded DNA (dsDNA) along with smaller structural components such as nucleosides have been used as stabilizing ligands in the production of AuNCs with tunable emission properties. In the case of adenosine-stabilized AuNCs, the delocalized electrons of the electron-rich N/O atoms or NH_2/OH functional groups involved in the surface of adenosine can be directly donated into the gold core *via* surface interaction, resulting in enhanced photoluminescence intensity and stability.[65]

One remarkable feature of DNA-NCs is the modulation of the emission fluorescence by changing the DNA-stabilizing sequence. Several DNA homopolymers of 30 units, including poly-adenosine A_{30}, poly-thymine T_{30} and poly-cytosine C_{30}, have been tested as stabilizers for DNA-AuNC synthesis. C_{30}-AuNCs synthesized at low pH showed strong blue fluorescence under UV light, which was higher than that obtained for A_{30}-AuNCs. In contrast, T_{30}-stabilized AuNCs exhibited almost no fluorescence (Fig. 3A and B). The influence of the DNA sequence in the AuNC emission properties was also evident when AuNCs were synthesized using various C-rich DNA sequences as stabilizing ligands. As shown in Fig. 3C, AuNCs formed with DNA containing 12 cytosines showed higher fluo-

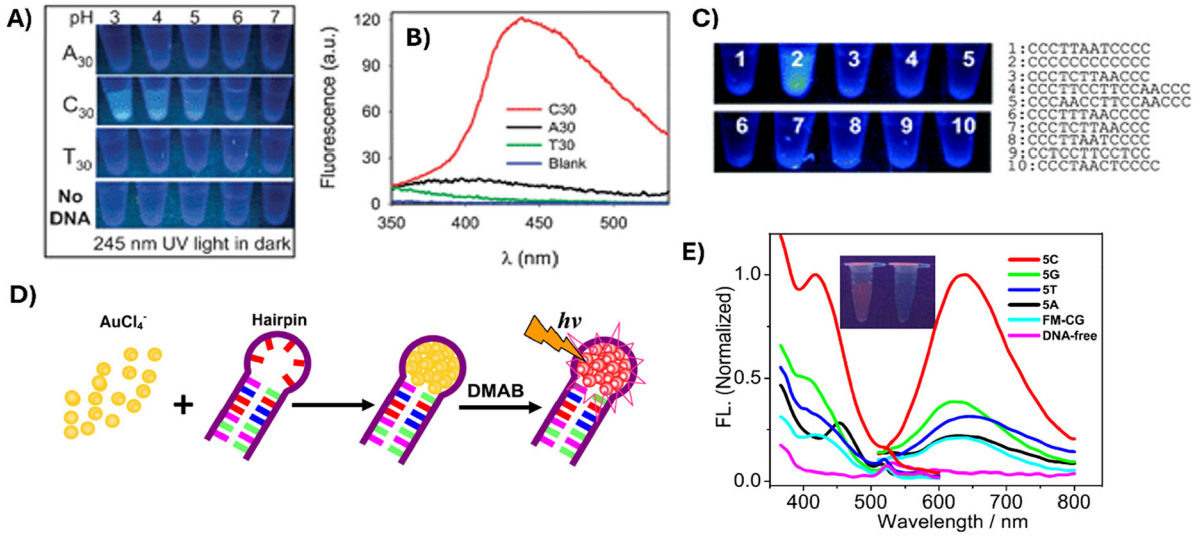

Fig. 3 Optical images (A) and fluorescence emission spectra (B) of Au-NCs templated by C_{30}, A_{30} and T_{30} sequences. (C) Optical images of AuNCs synthesized using various C-rich DNA sequences under UV light. Reproduced from ref. 66 with permission from the Royal Society of Chemistry, copyright 2012. (D) Schematic for the formation of fluorescent DNA hairpin-templated AuNCs. (E) Excitation and emission spectra of AuNCs obtained with different loop sequences. Inset: optical images of the solutions of DNA-AuNCs in the absence (right) and presence (left) of the 5C loop sequence under UV illumination. Reproduced from ref. 68 with permission from IOP Publishing, Ltd, copyright 2013.

rescence signals than those synthesized with other C-rich sequences.[66] The important role of A_{30} in the protection of the AuNCs *via* specific interactions with their nitrogen bases was demonstrated by Li and coworkers. They employed A_{30} as a protecting agent and UV light to promote the reduction of gold ions and obtained DNA-AuNCs with emission at 475 nm. A combination of AuNC nucleation sequence A_{30} with a 22-base recognition strand was employed to stabilize AuNCs, while allowing the hybridization with a complementary target DNA strand at the same time. Finally, they observed that the fluorescence of these dsDNA-AuNCs increased in the presence of the double-strand-chelating dye SYBR Green I (SG) due to interactions between the AuNCs and the dye. This work opened new possibilities to use such systems for the detection of specific nucleic acids in human serum.[67]

DNA hairpin structures, composed of a self-complementary double-stranded stem region and an unpaired loop part, have also been used to stabilize AuNCs (Fig. 3D). Interestingly, Liu and coworkers conducted a study investigating the role of the DNA sequences within the hairpin structure in the formation of fluorescent AuNCs.[68] They found that AuNC emission properties are highly dependent on the loop sequences. Thus, DNA loops with higher contents of cytosines stabilized the formation of AuNCs and also presented higher emission properties than guanine, thymine, or adenine-containing loops (Fig. 3E).

More complex structures such as self-assembled DNA molecules forming nanoribbons were employed by Ouyang *et al.* to biosynthesize nanoribbon-DNA-AuNCs.[69] The assembly of AuNCs in the DNA structure was performed intracellularly and resulted in a biohybrid material that was brighter and more stable than that synthesized in the absence of the nanoribbon template. Due to its enhanced stability, this system was successfully applied in long-term cellular tracking.

Another example of the use of AuNCs as fluorescent probes was reported by Bain *et al.*[70] In this work, they used fluorescence resonance energy transfer (FRET) to study with high spatial resolution the conformational changes of dsDNA in the presence of Ag^+ ions. DNA attached to AlexaFluor 488 acted as the donor, and AuNCs as the acceptor. Interestingly, it was found that the DNA length decreased from 9.8 to 8.3 nm in the presence of Ag^+ ions by the formation of Ag^+–C (cytosine) metal base pair bonds.

In addition to the photoluminescence properties, catalytic activities have been reported for DNA-AuNCs. In this sense, Chakraborty and coworkers demonstrated that the formation of a composite based on DNA-Au_7NCs (7 Au atoms) and bilirubin oxidase (BOD) using single-walled carbon nanotubes (CNTs) as support materials improves the electrocatalytic oxygen reduction reaction (ORR) compared with the BOD alone. In this case, Au_7NCs act as an enhancer of the electron transfer and lower the overpotential of ORRs.[71] In another example, theoretical studies were carried out to determine the catalytic potential of DNA-Au_3NCs for the oxidation of CO to CO_2. These studies demonstrated the potential of DNA-Au_3NC to act as a catalyst compared to pristine Au_3NCs.[72]

Another interesting research line is the study of proteins and DNA-AuNC interactions. The interaction with DNA-AuNCs can affect the secondary structure of the proteins and influence their biological function, as described by Zhai and coworkers.[73] They investigated the mechanism of interaction between DNA-AuNCs and human serum albumin (HSA), and found that the supramolecular interaction between HSA and DNA-AuNCs is spontaneous. Furthermore, using spectroscopy

techniques such Fourier-transformed infrared (FT-IR) and circular dichroism (CD), they demonstrated that the interaction of DNA-AuNCs and HSA promoted a change in the secondary structure of the proteins.

Strategies to enhance the photoluminescence quantum yield of biomolecule-stabilized AuNCs

Although AuNCs exhibit enhanced photostability compared with organic dyes and other fluorescent nanomaterials, their QYs are usually lower than those described for fluorescent dyes,[16,74] making their technological application challenging.

These reduced QYs arise from the effect of the biomolecular ligands on the electronic properties of the AuNCs. The biomolecules can provide electronic states that facilitate non-radiative transitions such as through energy transfer or charge transfer to the biomolecules, limiting the emission efficiency of the NCs. Hence, several strategies to improve the luminescence properties of biotemplated nanomaterials have been investigated. They include engineering the peripheral ligands on the NC surface, modifying the metallic core size, altering the core composition by alloying with hetero-metals, aggregation-induced enhancement, surface shell rigidification, self-assembling strategies, and regulating the ambient conditions such as temperature and solvents.[16]

GSH-AuNCs with a QY of 7% in water were synthesized using $NaBH_4$ as a reducing agent at pH 12. After addition of tetraoctylammonium (TOA) cations in toluene that interact with carboxylate anions of GSH, rigidification of the gold–thiolate shell is observed, remarkably enhancing the QY up to 60%.[75]

Aggregation-induced emission enhancement (AIEE) constitutes a well-documented strategy to enhance the photoluminescence of nanomaterials. By inducing aggregation, AuNCs stabilize in a confined state and radiative transitions of the AuNCs are reduced. Therefore, increasing the fluorescence emission QY leads to better performance of the AuNC-based systems. The aggregation degree can be controlled by fine-tuning the ligand charges and the pH of the solution.[76] Negatively charged heparin has also been used to connect positively charged GSH-AuNCs by electrostatic interactions, resulting in the aggregation of GSH-AuNCs and enhancement of the emission properties.[77] Similarly, an increase in the degree of confinement of BSA-AuNCs incorporated in micelles has been correlated with fluorescence enhancement, and interestingly, with changes in the α-helical character of the protein structure measured by CD.[78] Finally, GSH-AuNCs and Proline-AuNCs combined with cellulose allowed the obtention of hybrid materials with increased stability and enhanced fluorescence emission.[79]

Related to the modification of the metal core, a significant improvement in the QY has been achieved by incorporating metal atoms with higher electronegativity with the consequent change in the geometric and electronic structure of the metallic core.[80] The incorporation of lead(II) precursors in adenosine-stabilized AuNCs has been reported to have a dual effect, combining the structural rigidification of the AuNCs associated with the aggregation and the heavy-atom effect of lead. The resulting doped material exhibits enhanced emission properties.[65]

Chiroptical properties of AuNCs

Chirality is a common feature in Nature, which can be found at diverse scales, from molecules (*e.g.* DNA) to bigger systems (*e.g.* our hands). For this reason, the study of chirality in other fields such as nanotechnology has attracted the attention of scientific community. This type of system shows potential applications in different fields such as chiral sensing, catalysis and optoelectronics, among others.[81–83]

In the past few years, there has been a growing interest in the development and study of chiral AuNCs. From these studies, several types of chirality have been reported. In this section, we highlight the most common mechanisms for the formation of chiral AuNCs and some illustrative examples of chiral AuNCs protected by biomolecules (*e.g.* amino acids or DNA).

The preparation of chiral AuNCs can be summarized into two categories: (1) Formation of intrinsic chiral cores using achiral protecting agents; and (2) Achiral metal cores using chiral protecting agents.[84]

AuNCs with chiral cores using achiral protecting agents

Chiral AuNCs protected with achiral ligands exhibit chirality that arises from the AuNC core. In this context, achiral thiolated ligands[84] are the most commonly used molecules to obtain this type of chiral AuNCs. Different examples have been developed. For example, in $Au_{20}(SR)_{16}$ protected by 4-*tert*-butylbenzenethiolate (TBBT), the Au_7 inner core is achiral but the presence of the protecting TBBT units induces the chirality on $Au_{20}(SR)_{16}$.[85] Using the same TBBT ligand was possible to prepare other chiral NCs, $Au_{28}(SR)_{20}$ (SR = TBBT). In this case, the achiral AuNC core is formed by 20 gold atoms. Interestingly, the presence of four -SR-Au-SR-Au-SR induces the formation of an asymmetry obtaining chiral $Au_{28}(SR)_{20}$.[86]

The above-mentioned examples are based on Au–S interactions. Besides, Au–P interactions have been used to prepare chiral AuNCs. One example of that is $[Au_{20}(PP_3)_4]^{4+}$ where the core is based on Au_{13} and Au_7 and the interactions with the phosphine promote distortion of Au_7 introducing chirality on the Au_{20} core.[87]

Chiral AuNCs induced by the presence of chiral ligands

The chiroptical activity of AuNCs arises from their protection with chiral ligands. In this type of chirality, the presence of asymmetric ligands is necessary to promote chiral transmission information for obtaining chiroptical responses through the so-called *electronic ligand induction* mechanism.[84]

Using a dissymmetrically perturbed particle-in-a-box model, it was demonstrated that the chiroptical activity of AuNCs could arise from achiral metal cores perturbed by the presence of chiral fields from the asymmetric molecules (*e.g.* glutathione).[88]

For this reason, chiral biomolecules such as amino acids are excellent candidates to act as chiral coatings to AuNCs.[84] Cysteine, histidine, and GSH are the preferred biomolecules employed in chiral AuNC preparation. Chiral AuNCs can be used to distinguish enantiomers. In this sense, chiral AuNCs were employed by Garzón and coworkers to study the enantiospecific adsorption of cysteine. Their results demonstrated differences in the adsorption energies between L- and D-cysteine.[89] Chiral AuNCs (*ca.* 2 nm) protected with cysteine derivatives were developed by Gautier *et al.* In this work, they demonstrated that AuNCs show chiroptical responses due to the presence of chiral cysteines on their surface. Moreover, the interaction between the AuNC surface and carboxyl in addition to thiol groups was further demonstrated by Vibrational Circular Dichroism (VCD) experiments.[90] Interestingly, Kuo *et al.* reported that AuNCs protected by cysteine showed the ability to detect and inhibit the growth of *Escherichia coli* bacteria.[91]

One of the most interesting applications of chiral AuNCs is the chiral recognition. Several studies have been developed to investigate the potential specific interactions between chiral NCs and biological systems. In this context, Jiang and coworkers studied how the chirality of AuNCs protected with D-/L-cysteine affects the interaction with proteins (human coagulation factor XII and FXII) (Fig. 4A, B and C). Thus, they observed that D-AuNCs interact weaker than L-AuNCs with FXII. Thanks to this weak interaction with FXII, D-AuNCs can activate the protein for further cleavage.[92] Additionally, specific enantiomers of AuNCs demonstrated a strong influence on cells.[93] For example, chiral AuNCs loaded on racemic AuNP (size *ca.* 50 nm) films regulate the adhesion and differentiation of mouse bone marrow mesenchymal stem cells (MSCs). Interestingly, D-films showed better biocompatibility, higher cell density, and spreading area than L-films.[94] A similar enantiospecific effect has been described for other metallic NCs. For instance, Wang *et al.* demonstrated the specific action of L-NCs against resistance of *Pseudomonas aeruginosa* bacteria and higher cytotoxicity to mammalian cells compared to D-NCs.[95]

In another work, Heiz and coworkers prepared AuNCs with different sizes and good stability using L-Glutathione (L-GSH) and *N*-acetyl-L-cysteine (NALC) as stabilizing agents. Moreover, they demonstrated a chirality transfer phenomenon from the organic molecules to the metal core of AuNCs.[96]

Chiral transmission mechanism between cysteine derivative (*N*-isobutyryl-L(D)-cysteine, NIBC) and AuNCs describes the tunability of the chiroptical responses of NIBC-AuNCs. Thus, the introduction of polar protic solvents (*e.g.* water, ethanol) induces the self-aggregation of NIBC-AuNCs obtaining mirror optical activities. Furthermore, the use of non-protic polar solvents (*e.g.* DMSO) does not induce self-aggregation (Fig. 4D

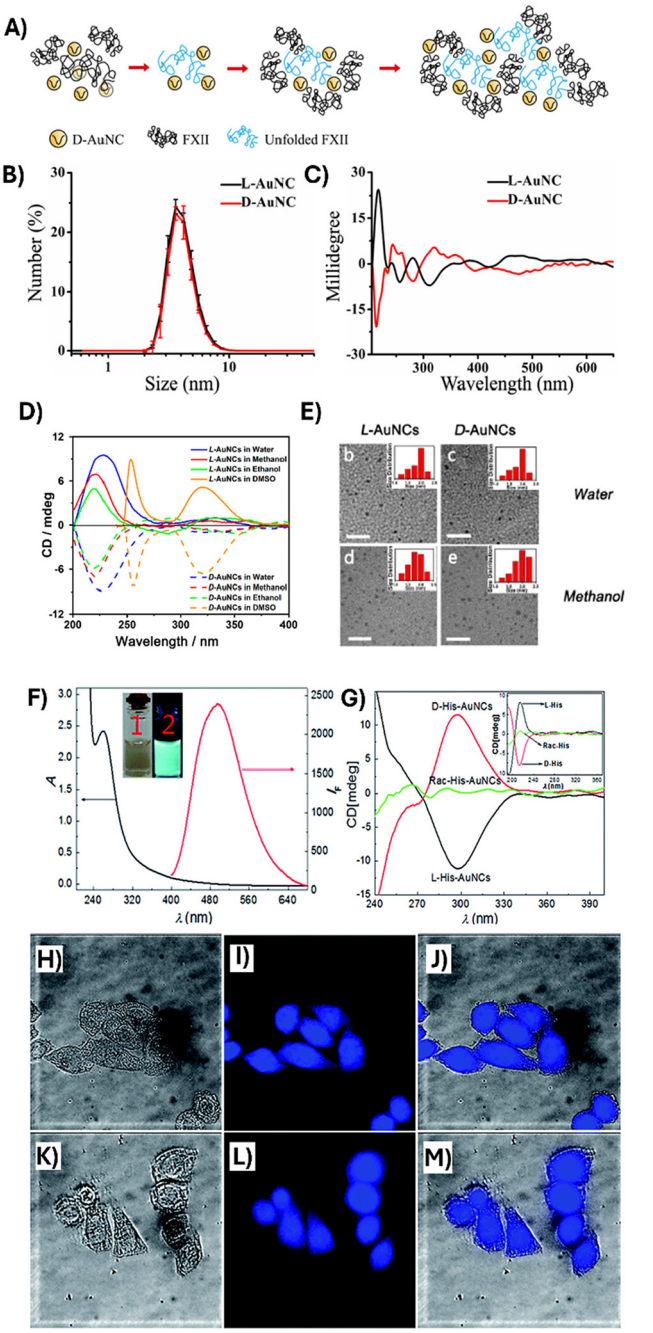

Fig. 4 Optical and chiroptical properties of chiral amino-acid-stabilized AuNCs: (A) schematic of the interaction between D-AuNCs and FXII. (B) DLS experiments of L- and D-AuNCs and (C) CD spectra of L- and D-AuNCs. Reproduced from ref. 92 with permission from Elsevier B.V., copyright 2021. (D) CD spectra of L- and D-AuNCs in different solvents. (E) TEM image of L- and D-AuNCs. Reproduced from ref. 97 with permission from the American Chemical Society, copyright 2019. (F) Absorption and emission properties of Histidine-AuNCs. (G) CD spectra of D-Histidine-AuNCs, L-Histidine-AuNCs and racemic Histidine-AuNCs. (H–J) Confocal images of Hep2cells in the presence of L-Histidine-AuNCs and (K–M) D-Histidine-AuNCs. Reproduced from ref. 100 with permission from the Royal Society of Chemistry, copyright 2015.

and E).[97] Tang *et al.* have demonstrated the different biosafety and pharmacokinetics of AuNCs when they are stabilized by D- or L-glutathione. In this work, they report that D-AuNCs present less cytotoxicity, hemolysis, and high tumor accumulation than L-AuNCs.[98]

D-/L-/DL-Histidine is also used as a protecting agent of AuNCs, and the influence of the chirality on the antibacterial activity was studied. In this sense, Zheng and coworkers demonstrated that the antibacterial activity against *Staphylococcus aureus* of D-AuNCs was more potent than that of L-/DL-AuNCs. This difference in the antibacterial activity is due to a decreased interaction of L- and DL-AuNCs with the bacterial cell components diminishing their efficacy.[99] Qi and coworkers used L-/D-histidine to obtain a chiral hydrogel-AuNCs with enhanced emission properties. Histidine transferred its chiral information to the hydrogel based on achiral thiobarbituric acid AuNCs using supramolecular interactions such as π-π stacking and hydrogen bonding. In another example, Guo *et al.*[100] have reported the preparation of chiral AuNCs using histidines as reducing and chiral protecting agents. In this work, the use of L- or D-histidine enantiomers allowed us to obtain blue-green emitting AuNCs with opposite chiroptical responses. Furthermore, they demonstrated no differences in the subcellular localization between L- and D-histidine-AuNCs (Fig. 4F–M).

Applications of biomolecule-stabilized AuNCs

Biosensing

Biomolecule-stabilized AuNCs have become valuable tools in biosensing because their optical properties, especially photoluminescence, are highly related to the local environment on the surface of AuNCs. Consequently, the interaction with target analytes impacts the emission properties of the AuNCs, which can be therefore used as efficient reporters for sensing applications. Small molecules, ions, and proteins are some of the reported targets in which the sensing system relies on the modulation of fluorescence emission of AuNCs (Fig. 5). Regarding ion sensing, sensitive detection of Cobalt has been achieved by measuring the quenching of fluorescence of green-emitting GSH-AuNCs.[33] In this system, Co^{2+} binds to sulphur atoms of GSH-AuNCs, disturbing the charge transfer process between the ligand and the Au core, thus decreasing the emission of GSH-AuNCs. The same quenching principle has been applied for the sensitive detection of copper ions using peptide,[54] amino acid,[30] or protein-stabilized[101] AuNCs.

Another example of ion sensing is the cascade detection of Zn^{2+} and the vitamin B6 cofactor pyridoxal 5′phosphate (PLP) by a papain-stabilized-AuNC nanoprobe developed by Chaudhary *et al.*[42] Conjugation with PLP led to a modification of the initial red fluorescence of the AuNCs to orange, with an emission band appearing at 525 nm and concomitantly quenched at 700 nm, presumably due to the formation of an imine linkage between the free $-NH_2$ groups of the papain stabilized NCs and the aldehyde in the PLP. Once conjugated with the PLP, the probe was used for the detection of Zn^{2+}, demonstrating its selectivity in the presence of interfering metal ions and in real environmental water samples. The detection mechanism was based on the alteration in the fluorescence emission color and profile, leading to a blue-shift and a 3-fold intensity enhancement triggered by the complexation-induced aggregation of the NCs. AuNCs have also been used for the detection of other target molecules, as tested by Cai *et al.*, using tryptophan-protected blue-emitting AuNCs that suffered quenching of fluorescence in the presence of furaltadone, allowing for naked-eye visual fluorescence determination of the presence of this antibiotic.[29]

Interestingly, the sensing capabilities of these systems can go beyond the detection of single molecules up to the study of enzymatic activities and even the differentiation of heterogeneous samples, constituting useful tools for diagnostics. Yang *et al.* prepared AuNCs using L-tyrosine both as a stabilizing ligand and as a reducing agent and used them to detect tyrosinase (TR) activity. The sensing principle was based on TR-induced fluorescence quenching of Tyrosine-AuNCs, due to the aggregations of Tyrosine-AuNCs on active sites of TR during the catalysis reaction.[31] Xu *et al.* synthesized AuNCs protected by CMMMMM peptides and used them for the detection of not only 10 separate proteins, but also for complex mixtures with subtle differences between them. Furthermore, these specific sensors were applied to differentiate breast cancer, severe osteoarthritis and rectal cancer patient serums from those of healthy people.[38] Regulating the pH values allowed the authors to obtain peptides with different positive or negative charges, which were used to create a five-element sensor array. CMMMMM–Au interacts with target proteins *via* electrostatic and hydrophobic interactions, affecting their binding energy and fluorescence lifetime, which together with energy transfer between the system and the target proteins, led to unique fingerprint-like patterns that were analyzed through linear discriminant analysis (LDA) statistics, allowing single protein detection, as well as discrimination between different complex protein mixtures and even distinction between diseased patient and healthy individuals serums.

In addition to the fluorescence, other properties of the AuNCs can be exploited for sensing applications. An example is the AuNC-embedded dual-enzyme NPs developed by Lee *et al.* as an electrochemical sensor for glucose.[102] In this case, glucose oxidase (GOx) and horseradish peroxidase (HRP)-stabilized AuNCs were prepared and cross-linked together with BSA-AuNCs, leading to the formation of nanoparticles containing several units of both enzymes. The detection was based on a chain reaction, in which the GOx-AuNC component of the NP oxidized glucose to generate H_2O_2, which then reacted with the HRP-AuNC component. The physical proximity of the enzymes reduced the diffusion and decomposition of the H_2O_2 intermediate, while AuNCs' high conductivity allowed an enhanced electron transfer between the enzymes and the electrode.

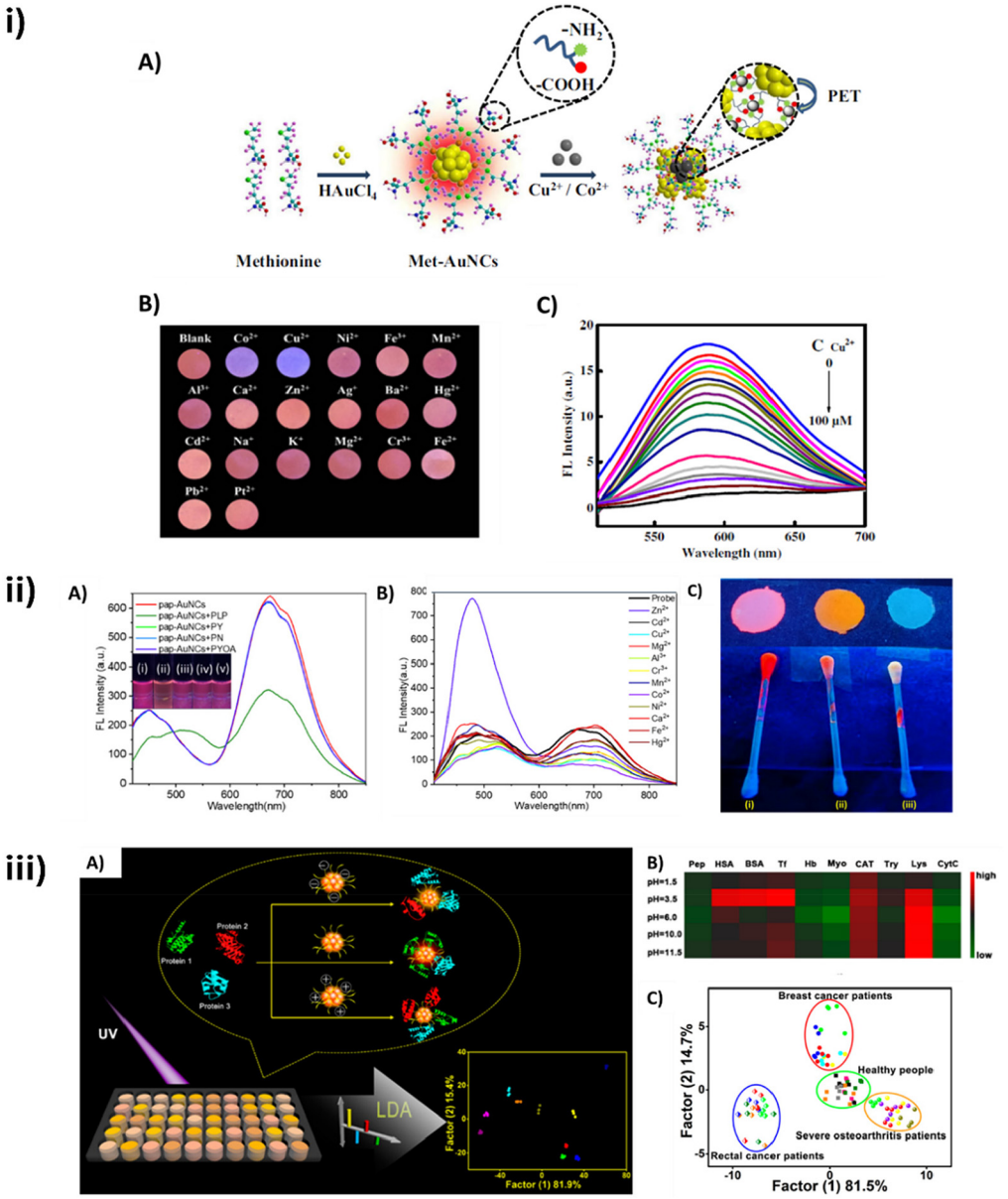

Fig. 5 Application of biomolecule-stabilized AuNCs in biosensing: (i) Met-AuNCs for Co^{2+} and Cu^{2+} specific sensing. (A) Scheme of the formation of Met-AuNCs and used as a fluorescent probe for the detection of Cu^{2+} and Co^{2+}. (B) Photographic images of Met-AuNC-based fluorescent test papers exposed to various ions. (C) Fluorescence spectra of Met-AuNCs after the addition of Cu^{2+} at different concentrations within 0–100 μM. Reproduced from ref. 30 with permission from Springer Nature, copyright 2019. (ii) Papain-AuNCs for the detection of Zn^{2+} and PLP. (A) Fluorescence spectral changes of pap-AuNCs in the presence of various VitB6 cofactors. (B) Fluorescence spectral changes of the PLP-pap-AuNCs probe in the presence of different metal cations (50 μM). (C) Paper strips and cotton buds coated with (i) pap-AuNCs, (ii) PLP-pap-AuNCs, and (iii) PLP-pap-AuNCs in the presence of Zn^{2+} ions. Reproduced from ref. 42 with permission from Springer Nature, copyright 2024. (iii) Peptide-AuNCs for protein and serum discrimination. (A) Schematic of the CMMMMM–AuNC-based sensor array for protein discrimination. (B) Pattern recognition of proteins using CMMMMM–AuNC-based sensor array. (C) Canonical score plot for the distinguishing results of serum from different diseases and healthy people. Reproduced from ref. 38 with permission from the American Chemical Society, copyright 2019.

Imaging and theranostics

AuNCs present a high photostability compared to organic dyes, which tend to suffer from photobleaching offering long-lasting and reliable labelling, constituting useful tools for imaging. Moreover, when stabilized within selected biomolecules, they can display excellent biocompatibility, long blood circulation times and good renal clearance, making them suitable for biomedicine and *in vivo* applications. However, the efficient targeted delivery within the body, avoiding sequestration by the liver and spleen, remains a challenge. While for tumor treatment and imaging, enhanced per-

meability and retention (EPR) effects play a key role, targeted strategies are also emerging as more controlled delivery alternatives for cancers, as well as for other diseases. In this sense, biomolecules play a key role to achieve selective delivery of AuNCs with promising features for bioimaging as they can be either selected from nature or engineered to have affinity for certain key molecules implied in disease processes, for example, by the addition of binding domains within the protein scaffolds.

As a demonstration of this difference between targeted and non-targeted delivery for bioimaging applications, ^{68}Ga-doped glutathione-coated AuNCs (^{68}Ga-GSH@AuNCs), and ^{68}Ga-labelled AuNCs with glutathione and arginine-glycine-aspartate (RGD) peptide co-coating (^{68}Ga-RGD-GSH@AuNCs) were used by Zheng *et al.* to successfully image tumor sites in mice by positron emission tomography-computed tomography (PET/CT) detection taking advantage of the ^{68}Ga labelling.[103] Both formulations were able to efficiently accumulate in tumor sites. However, the accumulation of the RGD-coated formulation was more effective, as it was due to active targeting of the αvβ3 integrin receptor, while the accumulation of the ^{68}Ga-GSH@AuNCs was mainly through ERP effects. Moreover, both presented good physiological and radiochemical stability, and could escape sequestration by the liver and spleen.

Focusing on the bioimaging specifically based on the AuNC intrinsic optical properties, the example is the use of DNA-stabilized AuNCs for cell imaging. In particular, a thiolated Mucin-specific aptamer employed as a scaffold yielded red-emitting AuNCs, with high biocompatibility and stability over a wide pH range. The fluorescent aptamer-AuNCs were used to effectively target breast cancer cells overexpressing mucin.[104] As for the antibodies, HER-2 receptor-specific monoclonal antibody, Herceptin, approved for breast cancer treatment, was employed as the stabilizer for the synthesis of fluorescent AuNCs.[105] Despite using high pH conditions during the synthesis procedure, the antibody maintained the receptor-specific targeting ability. Therefore, fluorescent Herceptin-stabilized AuNCs were applied for *in vivo* targeting toward HER2 receptors. Strong fluorescence signals of Her-AuNCs could be detected at tumor sites in mice, compared with the low background signal, making Herceptin-AuNCs a suitable fluorescent probe for *in vivo* imaging.

Additionally, these AuNC imaging capabilities can be combined with different therapeutic effects, either coming from the AuNCs of the stabilizing biomolecules to create theranostic tools that are applicable in several therapeutic modalities. Yang *et al.* designed a theranostic nanoprobe based on AuNCs stabilized by the protein alpha-lactalbumin (α-LA) (Fig. 6).[106] This complex allowed the visualization of overall tumor extension in the body by CT and magnetic resonance imaging (MRI). CT imaging was based on the AuNC X-ray absorption, which is due to the high Z and K-edge of gold. Furthermore, the use in MRI was based on the paramagnetic behaviour described for this type of AuNCs, which according to the density functional theory (DFT) is presumably due to them possessing a magnetic doublet with an odd number of electrons in the ground state.[107] These same AuNCs also displayed NIR fluorescence when excited at a single wavelength in the visible spectra, which allowed for local imaging of tumor extension in the operating room for image-guided surgical resection. Moreover, the system showed complementary antitumoral therapeutic effects, as the unfolded structure of the

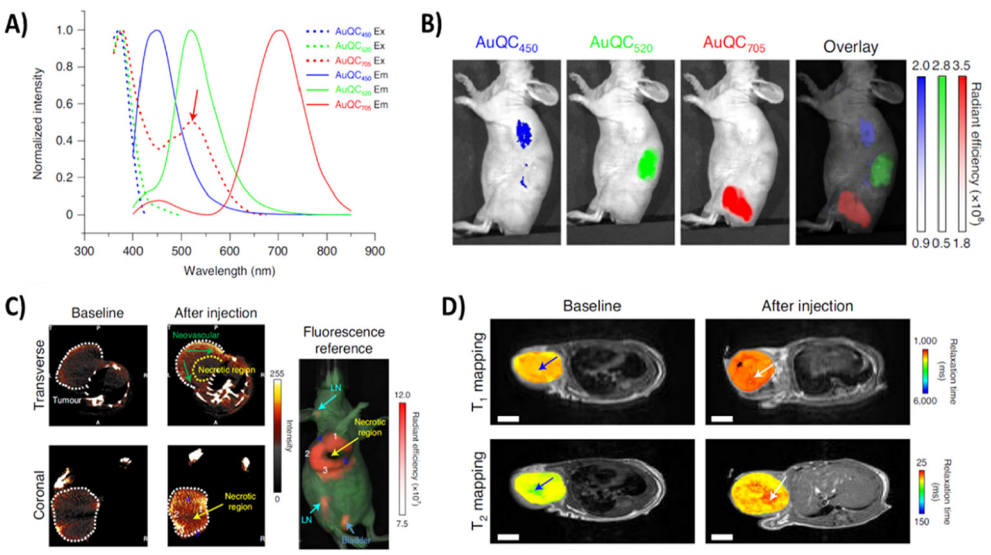

Fig. 6 Tumor imaging based on the properties of α-LA-stabilized AuNCs using different techniques. (A) Excitation (dotted lines) and emission (solid lines) spectra of AuNCs. (B) In vivo single-excitation multiplexing using α-LA-AuNCs in a J : NU mouse after subcutaneous injection. Excitation wavelength, 430 nm. (C) Coronal and transverse planar CT images of an MDA-MB-231 tumor after the injection of α-LA-AuNCs. (D) Two-dimensional transverse T1 and T2 maps of an MDA-MB-231 tumor superimposed onto anatomical MRI images after injection of α-LA-AuNCs. Reproduced from ref. 106 with permission from Springer Nature, copyright 2020.

protein helped the formation of lipoprotein complexes with oleic acid that triggered the inhibition of the MAPK and PI3K-AKT pathways, often associated with drug resistance in breast cancer. Similarly, Santhakumar *et al.* explored the use of two tripeptide-stabilized silver-doped AuNCs (TPGNCS) as photosensitizing agents for photodynamic therapy (PDT) (Fig. 7A).[108] Their long triplet-state lifetime favored excess reactive oxygen species (ROS) generation, triggering the loss of mitochondrial membrane potential and leading to apoptotic cell death. The systems simultaneously permitted cell imaging due to their strong red fluorescence, high QY, large Stokes shift, and good photostability.

An innovative alternative for the delivery of therapeutic NCs in tumors with a dense tumor microenvironment, such as pancreatic cancer, is the one presented by Schwartz-Duval *et al.*, who proposed a method for the *in vitro* and *in vivo* synthesis of fluorescent AuNCs through intracellular gold biomineralization for their use as radio-sensitizing agents, intensifying radiation damage to tumor cells in cancer radiotherapy (Fig. 7B).[109] This method uses Au(III) as a precursor, which, due to its reduced volume, uniformly diffuses through a desmoplastic tumor microenvironment and evades reticuloendothelial capture. Moreover, the authors observed that AuNC formation occurred more readily in tumor cells than in healthy ones, and that the particles colocalized mainly in the cell nuclei. The potential of these particles as radio-sensitizing agents is double. On the one hand, gold, because of its high atomic number transiently increases the radiation interaction probability of target tissues, probably due to the increase in photoelectric absorption interaction, followed by greater physical damage to tumor and endothelial cells. On the other hand, the AuNC synthesis itself perturbs cancer cell metabolism by modifying the relative abundance of metabolites that are involved in biomineralization. Redox metabolism including NADH metabolism, glutathione metabolism and the tricarboxylic acid (TCA) cycle was significantly perturbed by Au(III) treatment as ROS, reactive nitrogen species (RNS), glutamate, NADH, glutathione and citrate, which were reported to be involved in the reduction of Au(III) to Au(0). Moreover, imbalance of cellular redox status perturbs cell metabolism, accentuates peroxidation and affects nucleotide metabolism, leading to dysregulation of DNA repair after irradiation. The authors demonstrated the ability of this method to effectively alter tumor growth after radiation treatment in xerograph mouse models of pancreatic cancer. Treated mice also showed a longer survival than the untreated after radiation.

Biomolecule-AuNC hybrids offer the possibility of not only combining imaging and therapeutics, but also integrating more than one therapeutic modality in one system. An example of this is the development of nanocomposites that combined the fluorescence properties of AuNCs, the antibacterial activity of antimicrobial peptide (AMP) and the photothermal properties of conjugated polymers (CPs), by Zhu *et al.* (Fig. 7C). To build these systems, NPs of the conjugated polymer PDPP-DBT (CNPs) were first prepared. AMP, which is rich in amine, phenolic, and thiol groups, was directly modified on CNPs. Finally, upon NIR irradiation, Au ions were reduced and stabilized by AMP on the surface of CNPs. The

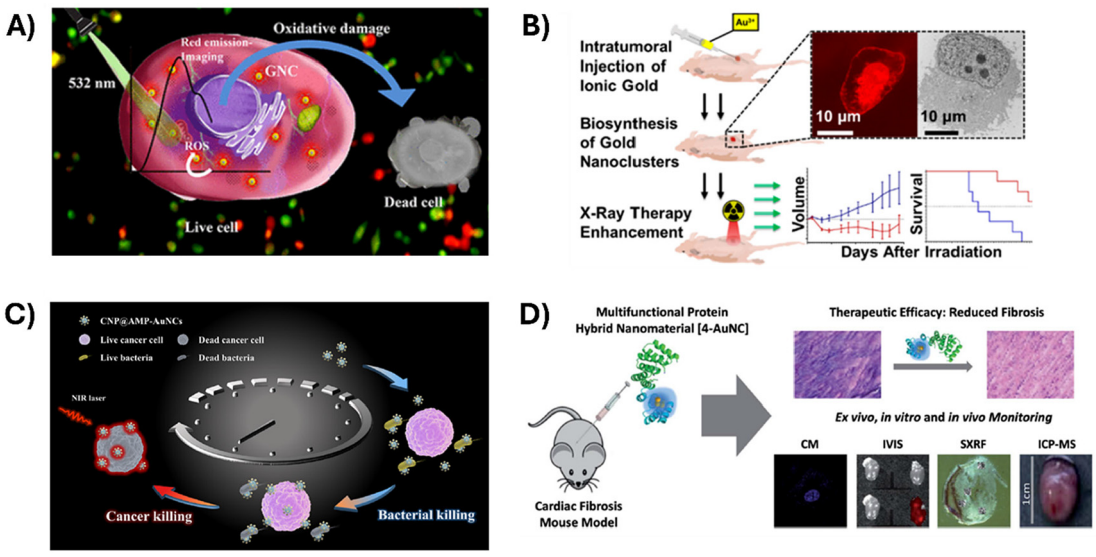

Fig. 7 Applications of biomolecule-stabilized AuNC-based theranostic agents. (A) Use of tripeptide-stabilized silver-doped AuNCs as photosensitizers for PDT by photoinduced generation of increased intracellular ROS. Reproduced from ref. 108 with permission from the American Chemical Society, copyright 2023. (B) AuNPs and fluorescent AuNCs synthesized by intracellular biomineralization used as radiosensitizers, increasing the radiation damage to cancer cells in radiotherapy. Reproduced with permission from ref. 109. (C) AMP-protected AuNCs conjugated to polymers applied as multivalent tools for combination therapies, integrating fluorescence imaging, antimicrobial activity, and photothermal cancer cell ablation. Reproduced from ref. 110 with permission from the American Chemical Society, copyright 2020. (D) Use of CTPR stabilized-AuNCs as target protein inhibitors in myocardial fibrosis. Reproduced from ref. 112 with permission from the Royal Society of Chemistry.

properties of the three components allowed us to treat cancer cells and bacterial infection while allowing cell imaging by fluorescence.[110] The antibacterial activity of AuNCs was also studied through DNase-stabilized AuNCs with photothermal properties. Bacteria biofilm elimination from medical devices was achieved by combining the DNase capability of breaking the biofilm matrix with the AuNC photothermal effect to promote a dispersion of bacterial biofilm up to 80% and killing 90% of the bacteria.[111]

Engineered proteins appear as promising versatile scaffolds to build multifunctional systems. An example is the design by Aires *et al.* of a CTPR with a therapeutic module able to bind and inhibit Hsp90 chaperone, a key protein in the cascade that triggers the overexpression of collagen related to myocardial fibrosis, and a nanomaterial-stabilizing module for the attachment of fluorescent AuNCs[112] (Fig. 7D). This system was successfully tested for the therapeutic intervention and monitoring of myocardial fibrosis in mice, along with the *ex vivo* and *in vitro* detection and imaging of heart tissue of treated animals by monitoring the gold nanoclusters, a metal not naturally found in biological systems, by synchrotron X-ray fluorescence (SXFR). This system was exploited further by RuizdelRio *et al.*[113] by the encapsulation of the newly developed CTPR-Au theranostic tool into extracellular vesicles (EVs) tagged with a far-red fluorescent protein to improve its biodistribution. EVs are nanometric particles containing a lipid bilayer and are used by cells to transport specific contents, playing an important role in cell-to-cell communication, both autologously and heterologously, making them excellent candidates for drug biotransportation. The colocalization of CTPR-Au and EVs inside NIH-3T3 cells was performed using fluorescence microscopy, demonstrating that the system could be internalized by the cells. Moreover, the quantification of Au in different organs by ICP-MS was used to study biodistribution in the *in vivo* models.

Industrial applications

Besides the medical field, the optical properties of biomolecule-stabilized AuNCs have a great potential for industrial applications. In particular, the use of these systems as bio-light-emitting devices (LEDs) has caught the interest of the scientific community, as their biomolecule templated synthesis offers a sustainable alternative to traditional white-emitting devices (WLEDs), often made of rare earth elements with toxic recycling procedures. Zetes *et al.* synthesized solid-state histidine-stabilized AuNCs (His-AuNCs) which exhibited a broad dual-band photoluminescence emission that covered a large area of the visible spectra region under UV irradiation, with fluorescence emission bands localized at 475 nm and 520 nm. The His-AuNCs showed an excellent purity of the generated white light while maintaining a high photo- and thermo-stability, proving their ability to perform as reliable WLEDs.[114] Moreover, Aires *et al.* used CTPR proteins to synthesize and stabilize blue- and red-emitting AuNCs simultaneously. These protein-AuNC hybrids were used to fabricate self-standing white light-emitting Bio-HLEDs, which after device optimization achieved a stability of over 800 h under working conditions. In addition, the chiral surrounding protein structure induced anisotropic emissions in the Bio-HLEDs, while allowing precise control of the size and place of AuNCs and shieling against photodegradation.[59]

Another promising application for biotemplated AuNCs in industries is the field of bioenergy and biofuels, using their high light-harvesting efficiency for energy conversion applications. As a proof of concept, Zhang *et al.* used fluorescent glutathione-templated AuNCs ($Au_{22}(SG)_{18}$) to achieve the photosynthesis of acetic acid from CO_2 in the non-photosynthetic bacterium *Moorella thermoacetica*, developing a photosynthetic biohybrid system that combined the catalytic performance of whole cell microorganisms and the light absorption efficiency of the AuNCs. The ($Au_{22}(SG)_{18}$) were internalized by the cells through passive targeting due to the glutathione's strong bioaffinity. When irradiated with simulated sunlight, photoexcited electrons from the AuNCs were transferred to cytoplasm-distributed redox mediators, entering the energy transfer system (ETS) and passing onto the Wood–Ljungdahl pathway to synthesize acetic acid from CO_2, while the holes were quenched by cysteine in glutathione. They demonstrated the usefulness of this system for solar-to-chemical energy conversion.[6]

Conclusions and perspectives

The enormous potential of AuNCs in different fields of applications such as biosensing, biotechnology, and biomedicine is undeniable, which inspired extensive research into their synthesis processes and the factors affecting the intrinsic properties of the nanomaterials.

The use of biomolecules such as amino acids, peptides, proteins, or DNA to generate bio-templated AuNCs has allowed the advancement of biotechnological and biomedical tools, due to the unique optical properties, high stability, solubility, and biocompatibility offered by the biohybrid NCs, as well as other functionalities. In this review, we highlighted a selection of the most recent advances in the preparation of biomolecule-stabilized-AuNCs, and the mechanisms behind the tunability of their (chiro)optical properties.

Tailoring of the optical properties of AuNCs such as absorption, fluorescence intensity, and emission wavelength can be achieved by ligand optimization, surface motif engineering, modification of the metallic core size and/or composition, and modification of the ligand's surrounding conditions. The latest research on this topic has evidenced the importance of understanding the effect of the ligand nature and its interactions with the NC, as well as the mechanisms governing the optical properties of AuNCs.

The main limitations of AuNCs stem from the significant impact of the stabilizing molecules on the surface of AuNCs, the interactions between the ligands and the core structure, and the interface with the external environment. These factors can influence their photophysical properties, which, in turn, affect their performance in various applications and hinder

their broader applicability. Achieving precise control over different processes that influence the optical and chiroptical properties of AuNCs is a pivotal challenge that must be addressed to overcome the potential weaknesses of these nanomaterials. Therefore, we can envision an increased interest in the development of customized hybrids to interrogate in a systematic manner and predict the impact of a given biomolecule used as AuNCs-ligand in the optical properties of the generated bionanomaterials.

For this aim, protein engineering has emerged as a promising approach, offering full control over the scaffold that interacts with the metals, thus enabling fine-tuning of the properties of stabilized AuNCs and expanding the range of these attractive hybrid nanomaterials, overcoming the limitations of natural proteins. Moreover, the ability to design biomolecules specifically to target molecules implicated in disease processes will enable the development of targeted theranostic tools that combine imaging capabilities with therapeutics, applicable across various therapeutic modalities.

Concerning chirality, the introduction of chiral biomolecules as protecting agents for AuNCs can simultaneously modify their optical (absorption and emission) and chiroptical properties, thereby endowing them with new functionalities. A deeper understanding and rational design of these components are therefore essential for developing such materials. For this reason, we anticipate that in the coming years, the relationship between chiral biomolecules and AuNCs and how this interaction influences the (chiro)optical properties of the nanomaterials will be explored in greater detail.

Overall, we found that future perspectives in the field include systematic and profound research to further correlate the properties of biological ligands and synthesis conditions with the physical and chemical properties of AuNCs. These studies would allow the development of customized ligands designed to adapt to the specific conditions of their intended applications. This approach allows for tightly controlled AuNC synthesis to achieve enhanced optical properties. Additionally, it facilitates the implementation of new functionalities introduced by the ligands, driving the creation of multifunctional hybrid gold-based nanomaterials with tailored capabilities. These materials can be further enhanced through approaches such as aggregation-induced enhancement, self-assembly strategies, and doping with other metals to improve their performance. Additionally, a deeper study on the interaction of these systems with cellular environments will be needed, both for biotechnological applications involving their use in bacteria and for biomedical applications. Enhancing the stability, maintaining the optical properties under physiological conditions, as well as controlling the ligand design to avoid the effects of intracellular metabolites, enzymes, and pH are some of the key challenges that should be addressed in coming years. Moreover, the applicability of AuNCs *in vivo* would benefit from extensive studies about metabolism, biodistribution, and toxicity.

We believe the use of biotemplated AuNCs in biomedicine and biotechnology will significantly expand in the following years. Notably, this includes the development of highly customized fluorescent sensors for environmental monitoring, gold-based contrast agents for imaging, nanomaterial-based therapeutics, or other innovative biological applications.

Furthermore, advanced applications such as chiral sensing, lighting devices, technological applications, and advanced photophysical sensors can benefit from these tuneable and chiral photoluminescent systems, broadening their impact across diverse fields.

Author contributions

Laura Saa: conceptualization, writing – original draft, writing – review & editing; Manuel Núñez-Martínez: writing – original draft, writing – review & editing; Eva Carpintero-Cueto: writing – original draft, writing – review & editing; Aitziber L. Cortajarena: conceptualization, writing – review & editing, funding acquisition. All authors have given approval to the final version of the manuscript.

Data availability

No primary research results have been included and no new data were generated or analysed as part of this review.

Conflicts of interest

There are no conflicts to declare.

Acknowledgements

A. L. C. acknowledges financial support from the from the European Union's Horizon Europe Research and Innovation Programme (Grant Agreement No. 101091980, 101046920, 964995, 964248, 964593 and 101131111), and the European Research Council – Grants (ERC-2022-PoC1-NanoImaging-101069356; ERC-2018-PoC-NIMM-841063). A. L. C. acknowledges support by the Spanish State Research Agency Grants TED2021-131641B-C41, PDC2021-120957-I00, PDC2022-133345-I00, and PID2022-137977OB-I00 funded by MCIN/AEI/10.13039/501100011033, the "European Union NextGenerationEU/PRTR", and "ERDF A way of making Europe". E. C-C. acknowledges the Spanish State Research Agency Grant for the FPI grant PREP2022-000553 (PIC2022-137877OB-100) funded by MCIN/AEI/10.13039/501100011033 and "ESF+".

References

1 Y. Chen, M. L. Phipps, J. H. Werner, S. Chakraborty and J. S. Martinez, *Acc. Chem. Res.*, 2018, **51**, 2756–2763.
2 G. Liu, Y. Shao, K. Ma, Q. Cui, F. Wu and S. Xu, *Gold Bull.*, 2012, **45**, 69–74.

3 S. Kundu, D. Mukherjee, T. K. Maiti and N. Sarkar, *ACS Appl. Bio Mater.*, 2019, **2**, 2078–2091.
4 H. Cui, Z. S. Shao, Z. Song, Y. B. Wang and H. S. Wang, *J. Mater. Chem. C*, 2020, **8**, 14312–14333.
5 G. Li and R. Jin, *Acc. Chem. Res.*, 2013, **46**, 1749–1758.
6 H. Zhang, H. Liu, Z. Tian, D. Lu, Y. Yu, S. Cestellos-Blanco, K. K. Sakimoto and P. Yang, *Nat. Nanotechnol.*, 2018, **13**, 900–905.
7 Y. Cong, X. Wang, H. Bai, C. Yao, J. Liu, Y. Wei, Y. Kang, S. Wang and L. Li, *Angew. Chem., Int. Ed.*, 2024, **63**, e202406527.
8 Y. Bao, H. C. Yeh, C. Zhong, S. A. Ivanov, J. K. Sharma, M. L. Neidig, D. M. Vu, A. P. Shreve, R. B. Dyer, J. H. Werner and J. S. Martinez, *J. Phys. Chem. C*, 2010, **114**, 15879–15882.
9 C. Zeng and R. Jin, *Chem. – Asian J.*, 2017, **12**, 1839–1850.
10 B. Zhang, J. Chen, Y. Cao, O. J. H. Chai and J. Xie, *Small*, 2021, **17**, 2004381.
11 Y. Wang and T. Bürgi, *Nanoscale Adv.*, 2021, **3**, 2710–2727.
12 Q.-F. Zhang, P. G. Williard and L.-S. Wang, *Small*, 2016, **12**, 2518–2525.
13 Y. Yu, B. Y. L. Mok, J. Loh, Y. N. Tan, Y. Yu, L. Mok, X. J. Loh and Y. N. Tan, *Adv. Healthcare Mater.*, 2016, **5**, 1844–1859.
14 A. Beloqui and A. L. Cortajarena, *Curr. Opin. Struct. Biol.*, 2020, **63**, 74–81.
15 M. Zhu, C. M. Aikens, F. J. Hollander, G. C. Schatz and R. Jin, *J. Am. Chem. Soc.*, 2008, **130**, 5883–5885.
16 X. Kang and M. Zhu, *Chem. Soc. Rev.*, 2019, **48**, 2422.
17 G. Li and R. Jin, *Acc. Chem. Res.*, 2013, **46**, 1749–1758.
18 R. Jin, C. Zeng, M. Zhou and Y. Chen, *Chem. Rev.*, 2016, **116**, 10346–10413.
19 D. M. Chevrier, A. Chatt and P. Zhang, *J. Nanophotonics*, 2012, **6**, 064504.
20 K. G. Stamplecoskie and P. V. Kamat, *J. Am. Chem. Soc.*, 2014, **136**, 11093–11099.
21 S. Maity, D. Bain and A. Patra, *Nanoscale*, 2019, **11**, 22685–22723.
22 S. Zhu, X. Wang, Y. Cong and L. Li, *ACS Omega*, 2020, **5**, 22702–22707.
23 Z. Wu and R. Jin, *Nano Lett.*, 2010, **10**, 2568–2573.
24 S. Mussa Farkhani, P. Dehghankelishadi, A. Refaat, D. Veerasikku Gopal, A. Cifuentes-Rius and N. H. Voelcker, *Prog. Mater. Sci.*, 2024, **142**, 101229.
25 D. Hao, X. Zhang, R. Su, Y. Wang and W. Qi, *J. Mater. Chem. B*, 2023, **11**, 5051–5070.
26 S. Zhu, X. Wang, Y. Cong and L. Li, *ACS Omega*, 2020, **5**, 22702–22707.
27 E. J. Mattioli, B. Cipriani, F. Zerbetto, T. D. Marforio and M. Calvaresi, *J. Mater. Chem. B*, 2024, **12**, 5162–5170.
28 R. Bélteki, L. Kuklis, G. Gombár, D. Ungor and E. Csapó, *Chem. – Eur. J.*, 2023, **29**, e202300720.
29 Z. Cai, H. Li, X. Yang, M. Zhang, J. Guo, Y. Su and T. Liu, *Spectrochim. Acta, Part A*, 2024, **308**, 123748.
30 F. Sang, X. Zhang and F. Shen, *Microchim. Acta*, 2019, **186**, 373.
31 X. Yang, Y. Luo, Y. Zhuo, Y. Feng and S. Zhu, *Anal. Chim. Acta*, 2014, **840**, 87–92.
32 B.-Y. Wu, C.-W. Wang, P.-C. Chen and H.-T. Chang, *Sens. Actuators, B*, 2017, **238**, 1258–1265.
33 R.-X. Zhao, A.-Y. Liu, Q.-L. Wen, B.-C. Wu, J. Wang, Y.-L. Hu, Z.-F. Pu, J. Ling and Q. Cao, *Spectrochim. Acta, Part A*, 2021, **254**, 119628.
34 Y. Lin, P. Charchar, A. J. Christofferson, M. R. Thomas, N. Todorova, M. M. Mazo, Q. Chen, J. Doutch, R. Richardson, I. Yarovsky and M. M. Stevens, *J. Am. Chem. Soc.*, 2018, **140**, 18217–18226.
35 Q. Dai, Z. Zhang, B. Yu, X. Li, J. Li, Z. Qi, H. He, F. Huang and X. Wang, *Nano Res.*, 2023, **16**, 12207–12214.
36 L. Zanetti-Polzi, P. Charchar, I. Yarovsky and S. Corni, *ACS Nano*, 2022, **16**, 20129–20140.
37 Z. Wang, C. Tang, M. Huang, X. Rong, H. Lin, R. Su, Y. Wang and W. Qi, *Langmuir*, 2022, **38**, 14799–14807.
38 S. Xu, W. Li, X. Zhao, T. Wu, Y. Cui, X. Fan, W. Wang and X. Luo, *Anal. Chem.*, 2019, **91**, 13947–13952.
39 J. Xie, Y. Zheng and J. Y. Ying, *J. Am. Chem. Soc.*, 2009, **131**, 888–889.
40 R. Nakum, A. K. Ghosh, B. Ranjan Jali and S. K. Sahoo, *Spectrochim. Acta, Part A*, 2024, **313**, 124143.
41 K. A. Brzezicka, S. Serna and N. C. Reichardt, *Nanoscale Res. Lett.*, 2018, **13**, 360.
42 J. Chaudhary, A. Tripathi and S. K. Sahoo, *J. Fluoresc.*, DOI: **10.1007/s10895-024-03849-9**.
43 M.-J. Lee, J.-H. Choi, J.-H. Shin, J. Yun, T. Kim, Y.-J. Kim and B.-K. Oh, *ACS Appl. Nano Mater.*, 2023, **6**, 12567–12577.
44 M. H. Griep and N. M. Bedford, *J. Phys. Mater.*, 2020, **3**, 045002.
45 L. Chen, M. Gharib, Y. Zeng, S. Roy, C. K. Nandi and I. Chakraborty, *Mater. Today Chem.*, 2023, **29**, 101460.
46 Y. C. Hsu, M. J. Hung, Y. A. Chen, T. F. Wang, Y. R. Ou and S. H. Chen, *Molecules*, 2019, **24**, 1630.
47 J. M. Dixon and S. Egusa, *J. Am. Chem. Soc.*, 2018, **140**, 2265–2271.
48 D. M. Chevrier, V. D. Thanthirige, Z. Luo, S. Driscoll, P. Cho, M. A. Macdonald, Q. Yao, R. Guda, J. Xie, E. R. Johnson, A. Chatt, N. Zheng and P. Zhang, *Chem. Sci.*, 2018, **9**, 2782–2790.
49 Y. Sun, Z. Zhou, P. Peng, T. Shu, L. Su and X. Zhang, *Anal. Chem.*, 2023, **95**, 5886–5893.
50 X. Zhang, Z. Huang, L. Zhang and W. Yang, *Langmuir*, 2023, **39**, 6748–6755.
51 H. Ding, H. Li, X. Wang, Y. Zhou, Z. Li, J. K. Hiltunen, J. Shen and Z. Chen, *Chem. Mater.*, 2017, **29**, 8440–8448.
52 D. Selvan, P. Prasad, S. Crane, A. Abuhagr, R. Covington, K. Artyushkova, G. Ramakrishna and S. Chakraborty, *Analyst*, 2019, **144**, 3949–3958.
53 W. Zhong, M. Wen, J. Xu, H. Wang, L. L. Tan and L. Shang, *Chem. Commun.*, 2020, **56**, 11414–11417.
54 H. Zhuang, X. Jiang, S. Wu, S. Wang, Y. Pang, Y. Huang and H. Yan, *Sci. Rep.*, 2022, **12**, 6624.
55 J. Zang, B. Zheng, X. Zhang, P. Arosio and G. Zhao, *J. Nanobiotechnol.*, 2019, **17**, 79.

56 P. Couleaud, S. Adan-Bermudez, A. Aires, S. H. Mejías, B. Sot, A. Somoza and A. L. Cortajarena, *Biomacromolecules*, 2015, **16**, 3836–3844.
57 A. Aires, A. Sousaraei, M. Möller, J. Cabanillas-Gonzalez and A. L. Cortajarena, *Nano Lett.*, 2021, **21**, 9347–9353.
58 A. Aires, I. Llarena, M. Moller, J. Castro-Smirnov, J. Cabanillas-Gonzalez and A. L. Cortajarena, *Angew. Chem.*, 2019, **131**, 6280–6285.
59 A. Aires, V. Fernández-Luna, J. Fernández-Cestau, R. D. Costa and A. L. Cortajarena, *Nano Lett.*, 2020, **20**, 2710–2716.
60 E. Lopez-Martinez, D. Gianolio, S. Garcia-Orrit, V. Vega-Mayoral, J. Cabanillas-Gonzalez, C. Sanchez-Cano and A. L. Cortajarena, *Adv. Opt. Mater.*, 2022, **10**, 2101332.
61 Y. Bao, C. Zhong, D. M. Vu, J. P. Temirov, R. B. Dyer and J. S. Martinez, *J. Phys. Chem. C*, 2007, **111**, 12194–12198.
62 J. Liu, *TrAC, Trends Anal. Chem.*, 2014, **58**, 99–111.
63 Z. Yuan, Y. C. Chen, H. W. Li and H. T. Chang, *Chem. Commun.*, 2014, **50**, 9800–9815.
64 D. Schultz, R. G. Brinson, N. Sari, J. A. Fagan, C. Bergonzo, N. J. Lin and J. P. Dunkers, *Soft Matter*, 2019, **15**, 4284–4293.
65 Q. Zhuang, C. Zeng, Y. Mu, T. Zhang, G. Yi and Y. Wang, *Chem. Eng. J.*, 2023, **470**, 144113.
66 T. A. C. Kennedy, J. L. MacLean and J. Liu, *Chem. Commun.*, 2012, **48**, 6845.
67 Z.-Y. Li, Y.-T. Wu and W.-L. Tseng, *ACS Appl. Mater. Interfaces*, 2015, **7**, 23708–23716.
68 G. Liu, Y. Shao, F. Wu, S. Xu, J. Peng and L. Liu, *Nanotechnology*, 2013, **24**, 015503.
69 X. Ouyang, N. Jia, J. Luo, Le Li, J. Xue, H. Bu, G. Xie and Y. Wan, *JACS Au*, 2023, **3**, 2566–2577.
70 D. Bain, B. Paramanik and A. Patra, *J. Phys. Chem. C*, 2017, **121**, 4608–4617.
71 S. Chakraborty, S. Babanova, R. C. Rocha, A. Desireddy, K. Artyushkova, A. E. Boncella, P. Atanassov and J. S. Martinez, *J. Am. Chem. Soc.*, 2015, **137**, 11678–11687.
72 N. K. Jena, K. R. S. Chandrakumar and S. K. Ghosh, *J. Phys. Chem. C*, 2012, **116**, 17063–17069.
73 H. Zheng, P. Wan, S. Qi, H. Chen and H. Zhai, *New J. Chem.*, 2020, **44**, 14060–14066.
74 D. Cheng, R. Liu and K. Hu, *Front. Chem.*, 2022, **10**, 958626.
75 K. Pyo, V. D. Thanthirige, K. Kwak, P. Pandurangan, G. Ramakrishna and D. Lee, *J. Am. Chem. Soc.*, 2015, **137**, 8244–8250.
76 M. Madhu, W. Bin Tseng, Y. S. Chou, A. S. Krishna Kumar, C. Y. Lu, P. L. Chang and W. L. Tseng, *Anal. Chem.*, 2024, **96**, 9007–9015.
77 D. Liu, X. Guo, H. Wu and X. Chen, *Spectrochim. Acta, Part A*, 2024, **304**, 123255.
78 P. Roberts, J. K. Perry, R. K. Gupta, S. P. Karna and J. Frechette, *J. Phys. Chem. Lett.*, 2020, **11**, 10278–10282.
79 Y. Duan, S. Yu, S. Xia, L. Wang, Z. Zhao, H. Liu, H. Huang, H. Zhu, L. Wang and H. He, *Chem. Eng. J.*, 2024, **481**, 148677.
80 T. Li, Z. Wang, Y. Zhang and Z. Wu, *Nanomaterials*, 2022, **12**, 3837.
81 M. Lago-Silva, M. Fernández-Míguez, R. Rodríguez, E. Quiñoá and F. Freire, *Chem. Soc. Rev.*, 2024, **53**, 793–852.
82 E. Yashima, K. Maeda, H. Iida, Y. Furusho and K. Nagai, *Chem. Rev.*, 2009, **109**, 6102–6211.
83 K. Kumaranchira Ramankutty, *Nanoscale*, 2024, **16**, 11914–11927.
84 C. Zeng and R. Jin, *Chem. – Asian J.*, 2017, **12**, 1839–1850.
85 C. Zeng, C. Liu, Y. Chen, N. L. Rosi and R. Jin, *J. Am. Chem. Soc.*, 2014, **136**, 11922–11925.
86 C. Zeng, T. Li, A. Das, N. L. Rosi and R. Jin, *J. Am. Chem. Soc.*, 2013, **135**, 10011–10013.
87 X. Wan, S. Yuan, Z. Lin and Q. Wang, *Angew. Chem., Int. Ed.*, 2014, **53**, 2923–2926.
88 M. R. Goldsmith, C. B. George, G. Zuber, R. Naaman, D. H. Waldeck, P. Wipf and D. N. Beratan, *Phys. Chem. Chem. Phys.*, 2006, **8**, 63–67.
89 X. López-Lozano, L. A. Pérez and I. L. Garzón, *Phys. Rev. Lett.*, 2006, **97**, 233401.
90 C. Gautier and T. Bürgi, *J. Am. Chem. Soc.*, 2006, **128**, 11079–11087.
91 T.-K. Chang, T.-M. Cheng, H.-L. Chu, S.-H. Tan, J.-C. Kuo, P.-H. Hsu, C.-Y. Su, H.-M. Chen, C.-M. Lee and T.-R. Kuo, *ACS Sustainable Chem. Eng.*, 2019, **7**, 15479–15486.
92 F. Hao, F. Geng, X. Zhao, R. Liu, Q. S. Liu, Q. Zhou and G. Jiang, *NanoImpact*, 2021, **22**, 100321.
93 Y. Cong, J. Liu, J. Zhang, J. Wang, X. Wang and L. Li, *ACS Appl. Bio Mater.*, 2024, **7**, 2695–2703.
94 X. Kang, Y. Wang, X.-L. Cai, Y. Hua, Z.-H. Shao, X. Chen, X. Zhao and S.-Q. Zang, *J. Colloid Interface Sci.*, 2022, **625**, 831–838.
95 Z. Wang, Y. Tian, J. Hao, Y. Liu, J. Tang, Z. Xu, Y. Liu, B. Tang, X. Huang, N. Zhu, Z. Li, L. Hu, L. Li, Y. Wang and G. Jiang, *ACS Nano*, 2024, **18**, 7253–7266.
96 M. Farrag, M. Tschurl and U. Heiz, *Chem. Mater.*, 2013, **25**, 862–870.
97 Z. Ma, G. Gao, Z. Luo, X. Tang and T. Sun, *J. Phys. Chem. C*, 2019, **123**, 24973–24978.
98 H. Tang, Q. Li, W. Yan and X. Jiang, *Angew. Chem., Int. Ed.*, 2021, **60**, 13829–13834.
99 J. Lei, T. Zhang, L. Wang, H. Jiang, J. Wu and Y. Zheng, *Colloids Surf., A*, 2024, **683**, 133033.
100 Y. Guo, X. Zhao, T. Long, M. Lin, Z. Liu and C. Huang, *RSC Adv.*, 2015, **5**, 61449–61454.
101 A. Aires, E. Lopez-Martinez and A. Cortajarena, *Biosensors*, 2018, **8**, 110.
102 M.-J. Lee, J.-H. Choi, J.-H. Shin, J. Yun, T. Kim, Y.-J. Kim and B.-K. Oh, *ACS Appl. Nano Mater.*, 2023, **6**, 12567–12577.
103 B. Zheng, Q. Wu, Y. Jiang, M. Hou, P. Zhang, M. Liu, L. Zhang, B. Li and C. Zhang, *Mater. Sci. Eng., C*, 2021, **128**, 112291.
104 B. Feng, Y. Xing, J. Lan, Z. Su and F. Wang, *Talanta*, 2020, **212**, 120796.

105 X. Zhang, M. Chen, Y. Zhang, Y. Hou, Y. Wu, M. Yao, L. Li, L. Shi, T. Liu, B. Hu, H. Zhao, X. Li, J. Shi, B. Jia and F. Wang, *ACS Appl. Bio Mater.*, 2020, **3**, 7061–7066.
106 J. Yang, T. Wang, L. Zhao, V. K. Rajasekhar, S. Joshi, C. Andreou, S. Pal, H. Ting Hsu, H. Zhang, I. J. Cohen, R. Huang, R. C. Hendrickson, M. M. Miele, W. Pei, M. B. Brendel, J. H. Healey, G. Chiosis and M. F. Kircher, *Nat. Biomed. Eng.*, 2020, **4**, 686–703.
107 M. Hembury, C. Chiappini, S. Bertazzo, T. L. Kalber, G. L. Drisko, O. Ogunlade, S. Walker-Samuel, K. S. Krishna, C. Jumeaux, P. Beard, C. S. S. R. Kumar, A. E. Porter, M. F. Lythgoe, C. Boissière, C. Sanchez and M. M. Stevens, *Proc. Natl. Acad. Sci. U. S. A.*, 2015, **112**, 1959–1964.
108 H. Santhakumar, R. V. Nair, D. M. Govindachar, G. Periyasamy and R. S. Jayasree, *ACS Sustainable Chem. Eng.*, 2023, **11**, 2102–2114.
109 A. S. Schwartz-Duval, Y. Mackeyev, I. Mahmud, P. L. Lorenzi, M. Gagea, S. Krishnan and K. V. Sokolov, *ACS Nano*, 2024, **18**, 1865–1881.
110 S. Zhu, X. Wang, S. Li, L. Liu and L. Li, *ACS Appl. Mater. Interfaces*, 2020, **12**, 11063–11071.
111 Y. Xie, W. Zheng and X. Jiang, *ACS Appl. Mater. Interfaces*, 2020, **12**, 9041–9049.
112 A. Aires, D. Maestro, J. Ruiz, D. Rio, A. R. Palanca, E. Lopez-Martinez, I. Llarena, K. Geraki, C. Sanchez-Cano, A. V. Villar and A. L. Cortajarena, *Chem. Sci.*, 2021, **12**, 2480–2487.
113 J. RuizdelRio, G. Guedes, D. Novillo, E. Lecue, A. Palanca, A. L. Cortajarena and A. V. Villar, *Theranostics*, 2024, **14**, 176–202.
114 M. Zetes, A. M. Hada, M. Todea, L. I. Gaina, S. Astilean and A. M. Craciun, *Nanoscale Adv.*, 2023, **5**, 5810–5818.